



Measurement of the first Townsend ionization coefficient in a methane-based tissue-equivalent gas



A.R. Petri^a, J.A.C. Gonçalves^{a,b}, A. Mangiarotti^c, S. Botelho^a, C.C. Bueno^{a,*}

^a Instituto de Pesquisas Energéticas e Nucleares, Cidade Universitária, 05508-000 São Paulo, Brazil

^b Departamento de Física, Pontifícia Universidade Católica de São Paulo, 01303-050 São Paulo, Brazil

^c Instituto de Física - Universidade de São Paulo, Cidade Universitária, 05508-080 São Paulo, Brazil

ARTICLE INFO

Keywords:

First Townsend coefficient
Methane-based tissue-equivalent gas
Nitrogen
Carbon dioxide
Methane

ABSTRACT

Tissue-equivalent gases (TEGs), often made of a hydrocarbon, nitrogen, and carbon dioxide, have been employed in microdosimetry for decades. However, data on the first Townsend ionization coefficient (α) in such mixtures are scarce, regardless of the chosen hydrocarbon. In this context, measurements of α in a methane-based tissue-equivalent gas (CH_4 – 64.4%, CO_2 – 32.4%, and N_2 – 3.2%) were performed in a uniform field configuration for density-normalized electric fields (E/N) up to 290 Td. The setup adopted in our previous works was improved for operating at low pressures. The modifications introduced in the apparatus and the experimental technique were validated by comparing our results of the first Townsend ionization coefficient in nitrogen, carbon dioxide, and methane with those from the literature and Magboltz simulations. The behavior of α in the methane-based TEG was consistent with that observed for pure methane. All the experimental results are included in tabular form in the [Supplementary material](#).

1. Introduction

The main object of microdosimetry is the study of the distribution of the deposited energy in irradiated micro sites of tissues to improve the understanding of the mechanisms responsible for a variety of radiation effects [1]. The reference detector in experimental microdosimetry has hitherto been the tissue-equivalent proportional counter (TEPC), firstly conceived by Rossi and Rosenzweig [2]. According to the tissue-equivalence principle, the walls and filling gases of TEPCs should have elemental composition and mass stopping powers similar to that of human tissues [3]. Tissue-equivalent gaseous (TEG) mixtures, that also allow stable operation of proportional counters with high gas gain, have been obtained by combining carbon dioxide and nitrogen with methane or propane. In comparison with methane, propane TE mixtures have superior gas gain but are less tissue equivalent [3–5]. A methane-based TE gas (CH_4 – 64.4%, CO_2 – 32.4%, and N_2 – 3.2%) has been largely employed in TEPCs operated at low pressure scaled to simulate the real size of microscopic tissue sites, as well as to ensure the validity of the cavity-chamber principle [6]. Meeting these dosimetric requirements is also needed for correctly comparing with microdosimetric distributions obtained from Monte Carlo simulations of charged particles tracks. Since the interactions of electrons with matter are at the core of any charged particle transport

code, knowledge of electron-collision cross sections with their energy dependence in real tissues or in TEG mixtures is important.

A frequently used method to determine electron-collision cross sections at low energies is to adjust them to reproduce accurate and reliable data on transport parameters, like the first Townsend ionization coefficient (α), drift velocity and diffusion coefficients. The first Townsend ionization coefficient is also a key parameter for modelling the avalanche growth at high electric field strengths, an important aid in the design of proportional counters. Despite the relevance of the knowledge of electron transport parameters for both theoretical and experimental microdosimetry, there is a paucity of these data for tissue-equivalent mixtures based on propane or methane. In particular, regarding the methane-based TEG (CH_4 – 64.4%, CO_2 – 32.4%, and N_2 – 3.2%), to the best of our knowledge, there is only one set of experimental data on the pressure-normalized first ionization coefficient (α/p) published by Schmitz and Booz [7] using a cylindrical tissue-equivalent proportional counter. Theoretical results of both α/p and gas gain in cylindrical proportional counters filled with the methane-based TEG were obtained by Ségur et al. [8] via numerical solution of the Boltzmann equation and Monte Carlo simulations. According to them, in cylindrical geometry, significant discrepancies between non-equilibrium and equilibrium values of the gas gain, and therefore of the first Townsend ionization coefficient, mainly arise from

* Corresponding author.

E-mail address: cbueno@ipen.br (C.C. Bueno).

the steep gradient of the electric field in the vicinity of the anode, preventing the electrons from reaching an equilibrium state. This effect can be avoided altogether when the electron avalanche grows under a uniform electric field provided by a planar geometry with large parallel electrodes. For this reason, the majority of the experimental values of the first ionization coefficient available in the literature have been obtained in such a geometry using either the Steady State Townsend (SST) or the Pulsed Townsend (PT) techniques. The latter was employed in our previous works [9–11] to measure the α coefficient in isobutane, at atmospheric pressure, using a beam from a N_2 laser and a variant of a traditional resistive plate chamber (RPC) [12,13] designed to provide self-protection against sparks. With this setup, first ionization coefficients normalized to the gas density (α/N) in isobutane were measured as a function of the reduced electric field (E/N) extending over 145–200 Td, where no data were available before. Apart from the atmospheric pressure, the upper limit of this narrow span of E/N was imposed both by the onset of spark production and the presence of the voltage drop across the resistive electrode. As a consequence of this ohmic drop, the effective electric field strength is less than that expected from the external applied voltage and the gas gap between the electrodes. In our previous experiments, this side effect, also present in RPCs [14,15] and cylindrical resistive proportional counters [16–18], was corrected following the method published elsewhere [11], taking into account both the average avalanche current and the resistance of the electrode. Nevertheless, as the ionization coefficient is the most sensitive transport parameter to even small variations of the field strength, some effort has been made to mitigate the effects of the ohmic drop by reducing the avalanche current through strict control of the laser parameters, such as the repetition rate and the beam intensity, which was limited by using calibrated attenuators. Despite of being simple, this procedure is very time-consuming, since at least eight hours are needed to perform each set of measurements.

The considerations exposed above show that there is still room for improvements in the experimental apparatus to reduce the effect of the ohmic drop by decreasing the avalanche current and to extend the range of the electric field, so far covered, towards higher values of E/N . It has been accomplished in the present work by using a mini diaphragm vacuum pump to reduce the pressure of the gas that flows continuously through the chamber. This approach also broadens the application of our setup to gas mixtures of interest in microdosimetry due to the possibility of adjusting the gas pressure within the range usually employed in TEPCs. The improved apparatus was commissioned by measuring the gas density-normalized ionization coefficient (α/N) in pure nitrogen, carbon dioxide, and methane extending over the range $85 \text{ Td} \leq E/N \leq 285 \text{ Td}$. These experimental results were cross-checked with other data available in the literature, employing different measuring techniques, and with predictions from simulations as well. The overall agreement obtained corroborated the good quality of the setup and allowed to perform, for the first time in planar geometry, measurements of α/N in the methane-based TEG ($CH_4 - 64.4\%$, $CO_2 - 32.4\%$, and $N_2 - 3.2\%$).

2. Experimental procedure and setup

The apparatus used in this work is essentially the same described in detail in our previous papers [10,11]. Its core is a parallel plate chamber constituted by an aluminum cathode, set 1.5 mm apart from the anode made with a high resistivity ($2 \times 10^{10} \Omega\text{-m}$) glass slab glued on a brass plate to allow its polarization via a high voltage supply (Bertan® 225-30 R, with ripple of 0.002%). A pulsed beam from a nitrogen laser (MNL200-LD LTB®, 100 μJ at 15 Hz), with 337.1 nm wavelength and 15 Hz repetition rate, was focused at grazing incidence onto the cathode surface to produce the primary electron cloud. These electrons were accelerated towards the anode and, above the threshold electric field strength, they underwent ionizing collisions creating more free electrons and positive ions in a cascade process, known as avalanche.

Under this condition, the total integrated (i.e. electronic plus ionic) current (I) was measured with a digital electrometer (Keithley® 6517B, accuracy of 1.0% of reading +3 fA for currents up to 20 pA), directly connected to the cathode. To minimize input bias current and voltage burden on the electrometer, an offset adjustment procedure was performed before acquiring each series of data. For each E/N value, 300 independent readings of the current were collected and their average and standard deviation values registered. The same procedure was adopted to measure both the primary ionization (I_0) and the noise currents (I_n). As the main component of the electronic noise is expected to arise from the laser assembly, realistic I_n measurements were performed at each E/N value keeping the laser beam on and the shutter closed, just before measuring each corresponding ionization or avalanche currents. Net values of I_0 and I , as well as the gas gap thickness (d), were used to calculate α/N coefficients through the equation $\alpha = \ln(I/I_0)/d$ in the E/N range between 85 Td and 290 Td. We have assumed that the mentioned equation, despite being derived from the Steady State Townsend technique, still holds in the present work as long as the following requirements were met: (i) the time constant of the external chamber network was large enough to provide pulse current integration under the repetition rate of 15 Hz; (ii) an upper limit of the E/N range ($\approx 300 \text{ Td}$) was set to avoid significant differences between ionization rate (R_i) and the product αv_d of the first ionization coefficient (α) and the diffusion modified drift velocity (v_d). Indeed, for nitrogen at atmospheric pressure, the difference between R_i and αv_d , which are well defined for the pulsed and steady state techniques, respectively, is expected to be less than 6% at 300 Td. This statement has been supported by a theoretical study on the current induced by avalanche growth in nitrogen, carbon dioxide, methane, and the methane-based TE mixture, as demonstrated in next section.

Measurements were performed with nitrogen (99.995% – Air Products®), methane (99.995% – AGA®), carbon dioxide (99.9995% – Air Products®), and the methane-based TEG mixture ($CH_4 - 64.4\% + CO_2 - 32.4\% + N_2 - 3.2\%$) by using calibrated mass flow controllers (Edwards® 825) connected to a multi-channel flow controller unit (Edwards® 1605). A mini diaphragm vacuum pump (KNF® 816.1.2KT.45P) was connected to the chamber outlet to decrease the gas pressure from the atmospheric pressure (930 hPa) down to the lowest one (120 hPa) allowed by the mass flow controllers characteristics. An absolute pressure transducer (Honeywell® FP2000), calibrated in the range of 0–1015 hPa (0.25% accuracy), gave the filling gas pressure inside the chamber. Measurements were carried out at a room temperature of $(18 \pm 1)^\circ\text{C}$, kept with the aid of an air-conditioning system, and registered all-day long with a datalogger (Extech® RHT50).

The adoption of the atmospheric pressure (930 hPa) and of the lowest pressure allowed by the mass flow controllers (120 hPa) still permitted some overlap in the E/N range covered in each case. This choice enabled us to cross-check the agreement among α/N values gathered in different pressures at the same E/N , as well as against our previously published values [10,11]. To ensure that electric field strengths were unaffected by ohmic drop effects, calibrated attenuators were used to decrease both the laser beam intensity and, consequently, the avalanche current. By applying this experimental approach, the ohmic drop was kept below 1% of the applied voltage, even at atmospheric pressure for the highest E/N .

Regarding the accuracy of the α/N measurements, the combined instrumental uncertainties were estimated to be 1.5%, while the overall uncertainty was 15%, gauged from the maximum deviation of the results obtained in several runs at the same E/N value. The major contribution to the overall uncertainty originates, according to our investigations, from the restrictions imposed by the grazing incidence of the nitrogen laser onto the cathode. Despite of the low beam divergence, it is cumbersome to focus the beam and completely prevent some photons from hitting the borders of the electrodes (edge effects).

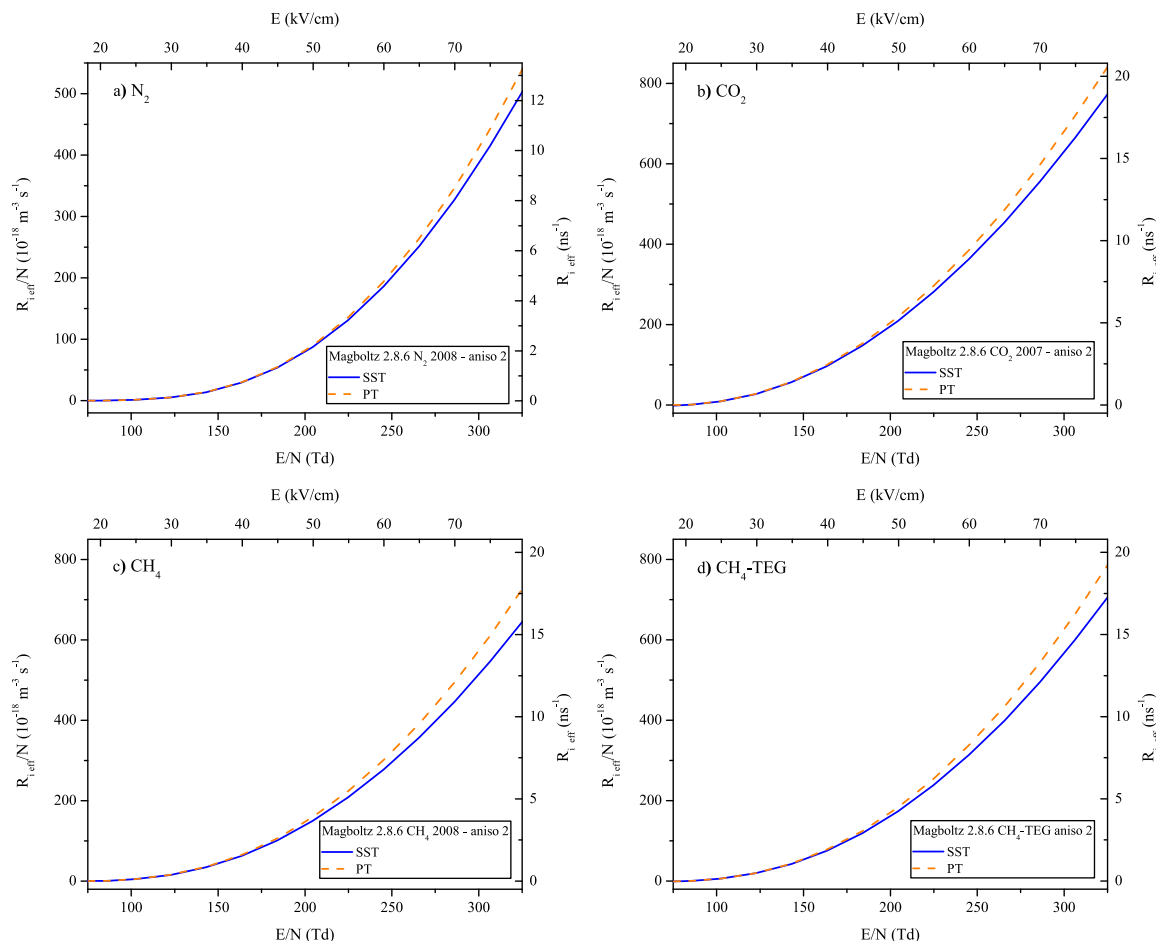


Fig. 1. Comparison of the PT ionization rate (R_i) with the product of the SST first ionization coefficient (α) and the SST diffusion modified drift velocity (v_d) as a function of E/N in: a) N_2 ; b) CO_2 ; c) CH_4 ; and d) CH_4 -TEG.

As a matter of fact, a difficult compromise has to be found on the transverse dimensions of the electrodes: the bigger they are the more uniform is the electric field in the gap, but, correspondingly, the more difficult it is to aim the laser at the central region where indeed such a larger uniformity can be profited. However, quantitative analyses of these sources of errors are not so straightforward. The value of the total uncertainty given here agrees with that claimed in our previous publications [10,11], estimated in the same way as the maximum deviation of the results obtained in several runs at the same E/N .

3. Simulations

3.1. Magboltz simulations

To calculate electron transport parameters, the publicly available Magboltz 2 code, developed by Biagi [19–22], was employed here. It is based on the Monte Carlo method and simulates individually each electron-molecule collision according to the appropriate integral cross section. Three processes are considered: 1) elastic collisions, 2) inelastic collisions resulting in the excitation of the molecule and 3) inelastic collisions resulting in the ionization of the molecule. In the last channel, it is necessary to describe how much of the kinetic energy of the impinging electron is transferred to the ejected one. Magboltz uses the analytic formula introduced by Opal, Peterson, and Beaty [23]. In all the three channels 1), 2), and 3), an accurate description mandates to include the angular anisotropies of the respective differential cross sections. Three options are available in Magboltz: isotropic cross sections (“iso”), anisotropic cross sections according to the parameterization introduced by Longo and Capitelli [24] (“aniso 1”),

and anisotropic cross sections according to the parameterization introduced by Okhrimovskyy et al. [25] (“aniso 2”). The default choice is “aniso 2”. For all gases implemented in the program, the number of levels included, the total cross sections and the constants needed in the parameterizations (we refer to all these information as the cross section set) have been adjusted by Biagi to best reproduce a selection of experimental data on electron transport parameters.

Here, in particular, we used version 8.6 of Magboltz 2, because it was available from our previous publications [9–11]. A comparison with older versions of Magboltz has been discussed in our previous work [10] and will not be repeated here. All simulations were run at atmospheric pressure and a temperature of 300 K. The total number of simulated collisions was of 10^{10} to reduce statistical uncertainties at the percent level even for the worst case of the diffusion coefficients (which were not used for the present work): the random fluctuations are completely negligible in the case of α . The results for α as a function of E were converted to α/N as a function of E/N .

For N_2 , two cross section sets are available: “ N_2 2004” and “ N_2 2008”. A comparison has been made in our previous work [10] and we do not repeat it. Here, we present the results of the simulations performed with the most recent set, i.e., “ N_2 2008”, which implements all the three options for the anisotropies of the cross sections: “iso”, “aniso 1”, and “aniso 2”.

For CO_2 , two cross section sets are implemented: “ CO_2 2004” and “ CO_2 2007”. The former only considers anisotropic cross sections with the Okhrimovskyy et al. [25] parameterization (“aniso 2”), while the latter implements all the three options: “iso”, “aniso 1”, and “aniso 2”. We show all four possibilities here. Because electron capture cross sections are implemented as well, i.e., the electronegativity is taken into

account, we actually report the effective first ionization coefficient given by the first ionization coefficient minus the attachment coefficient (the two are given separately by the program). At high values of E/N , this correction is not important; indeed it reaches above 5% only when E/N is below 180 Td.

For CH_4 , only one cross section set is available: “ CH_4 2008”, which implements all the three options for the treatment of the anisotropies: “iso”, “aniso 1”, and “aniso 2”. We show all three possibilities here. The electron capture cross sections are implemented also for this gas and once more we report the first ionization coefficient minus the attachment coefficient. However, we noticed that attachment changes α by more than 5% only when E/N is below 120 Td.

3.2. Ionization rate in SST and PT methods

To extend our method to field strengths higher than 200 Td, an investigation on the correspondence of the transport parameters obtained with the PT and SST techniques is required. As a matter of fact, the Magboltz code gives beyond α , the full set of transport parameters appropriate for both the SST and PT regimes. In the SST condition, the spatial growth of the avalanche is described by the first Townsend coefficient α ; while in the PT one, the ionization rate is the properly defined parameter. Such a difference has been pointed out by Sakai and Tagashira in two classical papers [26,27]. Here, see Fig. 1, as in a previous report [28], we compare the PT ionization rate (R_i) with the product αv_d of the SST first ionization coefficient (α) and the SST diffusion modified drift velocity (v_d) to give a quantitative estimate to the ambiguity in the definition of the transport parameters for our method, where we obtain α from the current growth in the PT regime. The differences at $E/N=300$ Td, about the maximum value reached by the present data, are 6.0%, 7.5%, 10.5%, and 9.5% for N_2 , CO_2 , CH_4 , and the TEG mixture, respectively. Since these values are still below the estimated overall uncertainty of the present data of 15% (see Section 2) or the systematic discrepancies between data sets from different authors of 20–30% (see Section 4), the difference of the transport parameters between the SST and PT regimes does not play a major role in the discussion of the results in Section 4.

4. Results and discussions

4.1. Validation of the setup and the PT ionization current method

Two aspects of the present work are new when compared to our previous publications [9–11]: the first is the use of lower pressures (below the atmospheric one) and the second is the application of the ionization current method, with a pulsed laser beam, at E/N values up to 300 Td (our previous work [10] stopped at 170 Td). Indeed they are connected: only the use of lower pressures has allowed us to reach a higher E/N limit before the ohmic drop in the anode and the background current, produced by discharges in the gap, started to affect the measurements. To validate the setup, first ionization coefficients were obtained with the quite extensively studied gas components of the CH_4 -based TE mixture: N_2 , CO_2 , and CH_4 . Measurements of α/N in these gases are plotted in the three panels of Fig. 2: they were carried out at atmospheric pressure (≈ 930 hPa) and 120 hPa, spanning the E/N interval from 85 Td to 285 Td. For each gas, the results were compared with the accurate data available in the literature, as well as with those expected from the simulations performed with the Magboltz code.

Our setup employs a parallel plate configuration to obtain a uniform electric field and avoid from the beginning, as much as possible, non-equilibrium effects; thus we choose as benchmark values from the literature only works where the same geometry was employed. Since experimental investigations on ionization coefficients in nitrogen for E/N below 200 Td are copious, for the sake of clarity, we restricted the number of authors cited herein mainly by removing duplicated data

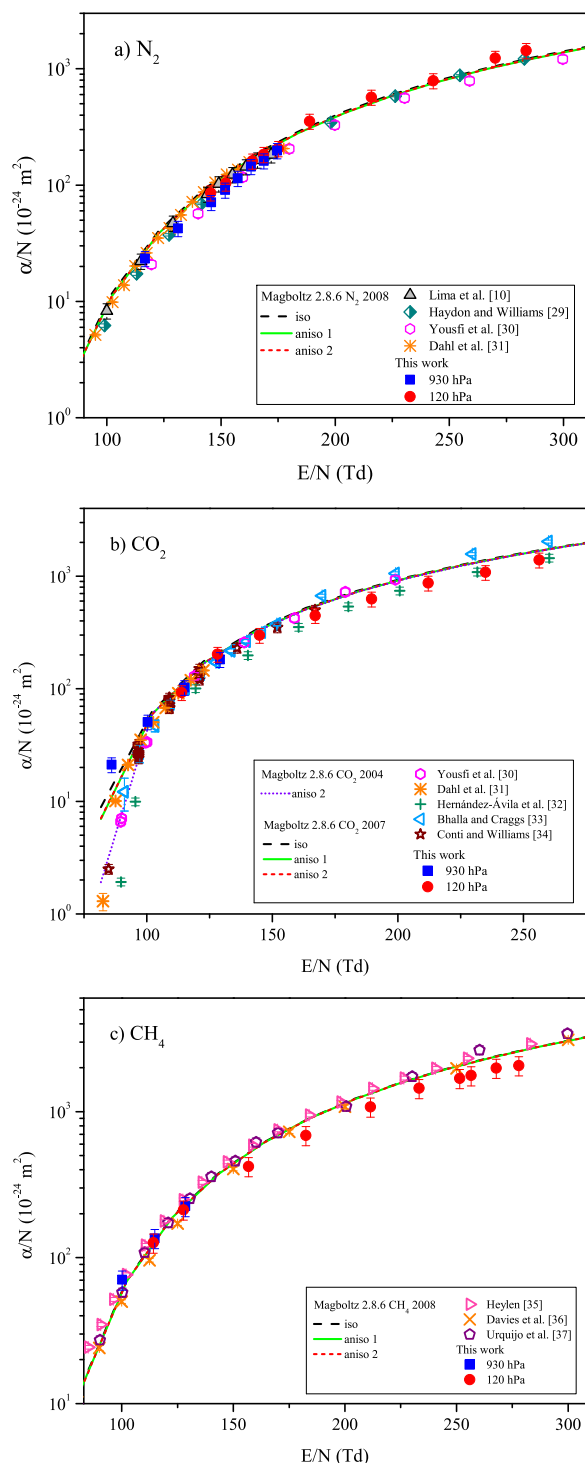


Fig. 2. Results of the density-normalized first ionization coefficient, α/N , as a function of E/N at both 120 hPa (bullets) and 930 hPa (squares) in: a) N_2 ; b) CO_2 ; and c) CH_4 . For comparison, data from the selected references (see Table 1) are also shown. Solid and dashed lines represent the results of simulations performed with the Magboltz code (see Subsec. 3.2 for more details).

sets (i.e. self-consistent ones published by the same research group). To help the reader, the selected references are shown in Table 1, with the relevant information about the method applied to obtain α/N , the availability of the results in tabular form, and its operational characteristics (i.e., the ionization source, the pressure and E/N ranges covered).

The experimental results obtained in the present work are made available in tabular form as Supplementary material. Each file refers to

Table 1

Relevant technical information of the references selected for the comparison among α/N data for each gas (N_2 , CO_2 , and CH_4) studied in the present work. Only measurements employing a planar geometry (i.e., a uniform filed configuration) have been chosen.

Authors	Year/Ref.	Method	Gas Gap (mm)	Pressure Range	E/N (Td)	Comments
Nitrogen – N_2						
Haydon and Williams	1976 [31]	SST	2–3	5,000 Torr (6.666 hPa)	85–3400	Rogowski copper electrodes. Hg lamp. Normal incidence. Tabulated values.
Yousfi et al.	2009 [32]	PT	30	0.6–600 Torr (0.8–800 hPa)	110–360	Electrodes 12 cm diameter. N_2 laser. Normal incidence.
Dahl et al.	2012 [33]	PT	9–18	10–110 hPa	50–180	Rogowski electrodes. 266 nm solid state laser. Normal incidence. Tabulated values.
Lima et al.	2012 [10]	PT	1.5	930 hPa	120–180	Resistive and aluminum electrodes. N_2 laser. Grazing incidence. Tabulated values.
This work		PT	1.5	100–930 hPa	115–285	Resistive and aluminum electrodes. N_2 laser. Grazing incidence. Tabulated values.
Carbon Dioxide - CO_2						
Bhalla and Craggs	1960 [35]	SST	up to 40	0.5–100 mmHg (0.67–133.3 hPa)	79–3643	Rogowski electrodes. Hg lamp. Normal incidence. Tabulated values.
Conti and Williams	1975 [36]	SST	2–30	14–667 Torr (19–889 hPa)	85–167	Copper cathode. Hg lamp. Normal incidence. Tabulated values.
Hernández-Ávila et al.	2002 [34]	PT	30	0.26–10 hPa	90–380	Electrodes 12 cm diameter. N_2 laser. Normal incidence.
Yousfi et al.	2009 [32]	PT	30	0.6–600 Torr (0.8–800 hPa)	90–200	Electrodes 12 cm diameter. N_2 laser. Normal incidence.
Dahl et al.	2012 [33]	PT	9–18	10–110 hPa	80–120	Rogowski electrodes. 266 nm solid state laser. Normal incidence. Tabulated values.
This work		PT	1.5	120 and 930 hPa	85–255	Resistive and aluminum electrodes. N_2 laser. Grazing incidence. Tabulated values.
Methane – CH_4						
Heylen	1963 [37]	SST	up to 12	0.5,3,30,200 Torr (0.67–267 hPa)	85–8500	Rogowski electrodes. UV light. Normal incidence. Tabulated values.
Davies et al.	1989 [38]	TOF	7 to 52	0.1–1000 Torr (0.13–1333 hPa)	80–1000	Drift tube. Pulsed Xe lamp. Tabulated values.
Urquijo et al.	1999 [39]	PT	35	0.133–66.7 kPa	70–700	N_2 laser. Normal incidence.
This work		PT	1.5	120 and 930 hPa	100–280	Resistive and aluminum electrodes. N_2 laser. Grazing incidence. Tabulated values.

one of the gases (or the gas mixture) considered and four columns are given: the first for the pressure, the second for E/N, the third for α/N , and the fourth for the total uncertainty on α/N .

The consistency among our data on α/N and those gathered from the articles presented in Table 1 was checked by plotting the logarithm of α/N as a function of N/E for N_2 , CO_2 , and CH_4 in Fig. 3. In fact, by using this representation, the behavior of the data points is expected to be almost linear, rendering the judgment of the overall agreement easier by eye. These results can indeed be fitted with the Korff parameterization [29,30], $\alpha/N=A \exp(-B \cdot N/E)$, where A and B are constants related to the gas, as it can be seen in Fig. 3.

The fair agreement among these different sets of experimental data for N_2 , CO_2 , and CH_4 can be quantified by analyzing their residues with respect to the Korff parameterization, as presented in Fig. 4. The A and B coefficients were determined by fitting all measurements (ours and those from the literature) together with the same weight (disregarding the quoted uncertainties owe to the different standards used by the authors for their uncertainty statements). In the case of CO_2 and CH_4 , the fit converged only when the lowest part of the covered E/N range was excluded (this will be discussed in more details below). The residues between the theoretical predictions by Magboltz to the Korff parameterization are also included in this figure for a later discussion. Since α/N changes by two to three orders of magnitude over the E/N range of interest here, depending on the gas considered, differences of the order of 20–30% cannot be appreciated on the logarithmic scale adopted in Figs. 2 or 3. The introduction of a residue plot, on the contrary, allows choosing linear scales. Although we reported error bars in all figures, only in the one with the residues they became clearly visible (this fact alone fully justifies the introduction of such a representation). For our data, we report two errors: one with a continuous bar and one with a dashed bar, representing the instrumental and overall uncertainties, respectively (see Section 2). For the other authors, we have reported their quoted total error with a continuous bar.

N_2 : The experimental data obtained in the present work in the E/N range between 115 Td and 285 Td are compared with those chosen from the literature in Fig. 2a. Irrespective of the method applied to obtain the data on α/N (i.e. SST or PT), all results are consistent with the Korff parameterization down to the multiplication threshold, as it is clearly visible in Fig. 3a: the fit converges when all the points displayed are included. The residues could then be defined for all of them and are represented in Fig. 4a. The results obtained for $E/N < 170$ Td agree with our previous data [10] within the total uncertainty claimed for the earlier measurements (15%), except for the last two points towards the highest electric field strengths. In this region, the somewhat larger discrepancy ($\approx 16\%$) is attributed to the ohmic drop across the resistive anode in the former setup. In the present work, even at high E/N, this side effect did not reduce the applied voltage by more than 1%, either at low (120 hPa) or atmospheric pressure (930 hPa) because attenuators were used to reduce the avalanche current, as discussed in Section 2. Indeed, α/N values gathered at the two different pressures but at rather close values of E/N agree within the total uncertainties ($\approx 15\%$) estimated in this work. For E/N above 200 Td, our measurements are about 20–30% above the others. An analysis of Fig. 1a reveals that this increase cannot be attributed to the difference between the ionization rate and the first ionization coefficient obtained from the PT and SST techniques, respectively. In fact, the agreement, within the quoted uncertainties, between the data by Haydon and Williams [31], obtained in a SST condition (see Table 1), and those by Yousfi et al. [32] (see Table 1), collected with a time-resolved pulsed Townsend technique, supports the conclusion that both methods give consistent results in the E/N range of interest here. Though, it is likely that our two measurements at the highest E/N were performed in the pre-breakdown region. In particular, these discrepancies with other authors are possibly due to the influence of secondary ionization on the measured ionization growth. The physical processes underlying this phenomenon were thoroughly investigated by Haydon and Williams

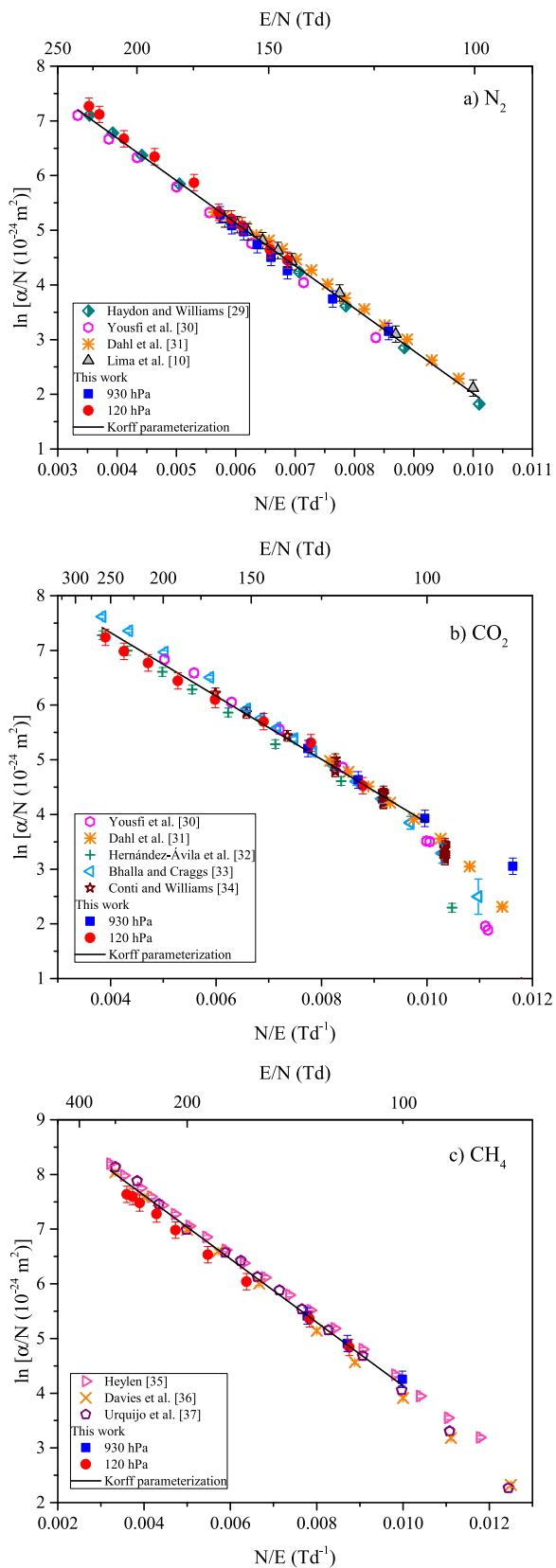


Fig. 3. Linearized representation of $\ln(\alpha/N)$ versus N/E for a) N_2 ; b) CO_2 , and c) CH_4 . The fit with the Korff parameterization to all the measurements (ours and those from the literature) is also shown by the continuous line. The same line also indicates the range considered for the fit (which is not the same for all panels, see the text for details).

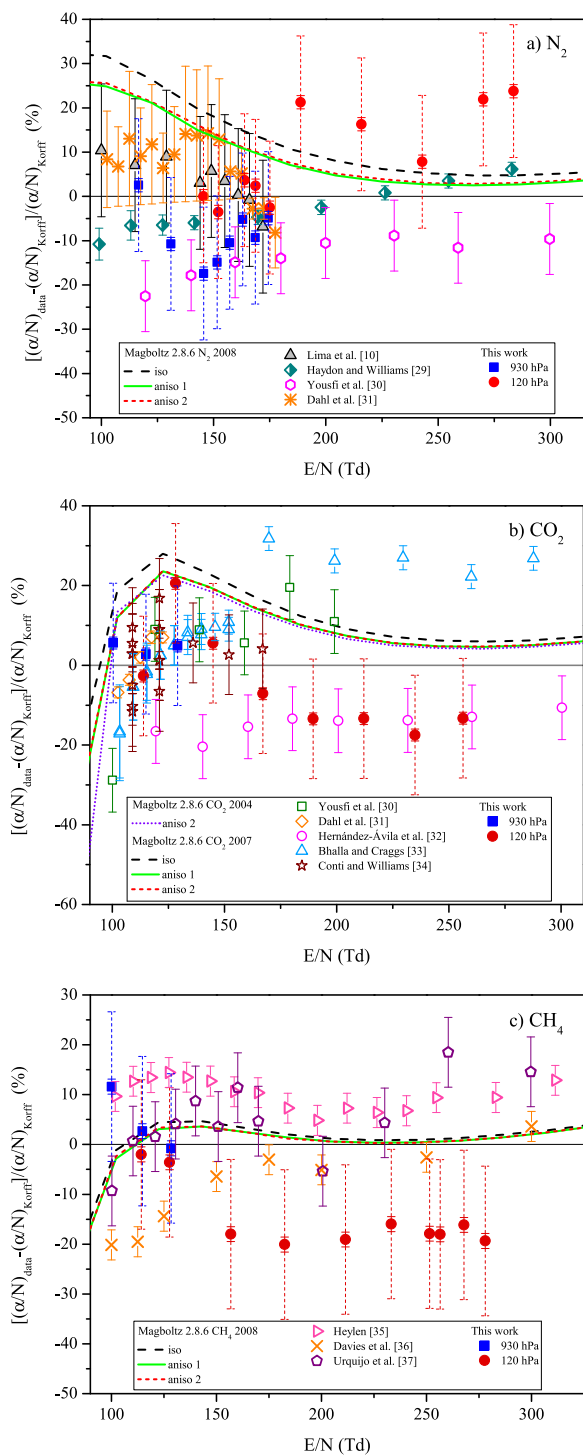


Fig. 4. Residues of the experimental data on α/N from the fit with the Korff parameterization for a) N_2 ; b) CO_2 ; and c) CH_4 . The residues of the Magboltz calculations are also shown (different cross section sets and different options for the description of their anisotropies are considered; see Subsec. 3.1 for more details). The error bars represent the total uncertainty (dashed line) and the instrumental uncertainty (full line).

[31]. They were able to find a self-consistent set of ionization coefficients which, as shown in Fig. 4a, match very well with the simulation within the whole range covered in this work. In conclusion, from the residues plotted in Fig. 4a, it can be seen that all data agree to within 20% in the full E/N range except our last two measurements, toward the pre-breakdown region, that rise more sharply (25%) than all other data.

The comparison between data and Magboltz simulations indicates a systematic overestimation of the latter by the former for reduced electric field strengths less than 175 Td (i.e., close to the threshold for avalanche multiplication). Possibly, small inaccuracies in the ionizations cross sections have a larger impact on the predicted α/N under such conditions. The inclusion of anisotropies in the cross sections reduce α/N by a quantity that increases, in absolute value, up to 6% towards lower E/N, while the details of the parameterization adopted is far less important over all the E/N range considered in the present work. This fact has been already observed in our previous publication [10], where we compared extensively the two different cross section sets available (see Subsec. 3.1), covering all options for the description of anisotropies and all transport parameters. Given the current situation visible in Fig. 4a, the experimental uncertainties, in particular the much larger systematic deviations between different publications, do not allow to make any definitive statement about the need to include anisotropies in the cross sections. The very good agreement between Magboltz simulation and the data by Dahl et al. [33], gathered at values of E/N < 180 Td, is also shown in this figure. Likewise, the results obtained by Yousfi et al. [32] for reduced field strengths between 110 Td and 360 Td agree within the experimental error with Magboltz calculations. The simulations do not follow a Korff parameterization down to very close to the multiplication threshold (the same trend is actually present for all gases and we do not repeat the present discussion for each of them). Once more, it is important to bear in mind that, under such conditions, the value of α/N is very small and any inaccuracy in the cross sections or in their energy dependence has a large relative effect. More thorough investigations would be necessary to identify the particular cross section responsible for the problem.

CO₂: Our data for α/N measured in the range of E/N between 85 Td and 255 Td are presented in Fig. 2b, together with the others available in the literature. For this gas, known to have attaching properties [34,35], our method, based on the net current growth, actually measures the effective ionization coefficient (ionization minus attachment). However, to avoid an excessive burden of notation, we maintain the symbol α and call it the first ionization coefficient. For E/N below 100 Td, large discrepancies have been found among different sets. The source of these difficulties is probably the experimental inaccuracy of the measurement of the ionization currents that are, unavoidably, very low near the threshold for avalanche multiplication (≈ 70 Td). Only our data at atmospheric pressure, contrary to the others, do follow a linear behavior in the representation of Fig. 3b down to the threshold: we have been forced to fit the Korff parameterization only in the region of E/N above 100 Td and, for such a reason, the horizontal scale of Fig. 4b can only begin at E/N=100 Td. In contrast, all sets of data on α/N extending over 100 Td < E/N < 175 Td are in excellent agreement, as it appears more clearly in the residue plot of Fig. 4b. Within this range of field strengths, it can be seen that our results obtained at either 930 hPa or 120 hPa, agreed within 11% at a rather close E/N values. In the region above 175 Td, the results seem to cluster along two lines, as visible again in Fig. 4b: the data by Hernández-Ávila et al. [34] and ours lie below the fit with the Korff parameterization (represented by the horizontal line) and those by Yousfi et al. [32] and by Bhalla and Craggs [35] lie above. Such a division between the experimental values does not follow the technique employed (only Bhalla and Craggs [35] and Conti and Williams [36], who stopped at lower E/N and actually lie in between the two previous clusters, employed the SST, see Table 1). Indeed, from the simulations presented in Fig. 1b, the differences between the regimes used are not enough to justify the mentioned discrepancies. In conclusion, it can be seen that all data obey the Korff parameterization over the E/N range from 100 Td up to 255 Td, the residues of each result to the Korff parameterization being smaller than 20%, with the exception of those by Bhalla and Craggs [35] at high electric field strengths (E/N > 175 Td), whose residues are almost 25%.

The Magboltz simulations follow the general trend of the data for E/N above 100 Td. Between 100 Td and 175 Td, the simulations actually

overestimate most of the measured points by approximately 10%, which is of the order of the estimated uncertainties. Above 175 Td, the theoretical values actually fall in between the two clusters of points mentioned: those by Hernández-Ávila et al. [34] and ours and those by Bhalla and Craggs [35] and Yousfi et al. [32]. Once more, because Magboltz stays in between, the differences are less than present systematic uncertainties. The inclusion of the anisotropies of the cross sections results in a reduction of α/N again of up to 6% at low E/N, while the details of the parameterization employed are hardly noticeable. The two cross section sets available (see Subsec. 3.1) also give very close results. Because the present discrepancies between different authors are four to five times bigger, it is not possible to use data on α/N to support experimentally the necessity to include the anisotropies of the cross sections (not to mention a particular cross section set) in the E/N range investigated here.

CH₄: The measured values of α/N are presented in Figs. 2c and 3c together with earlier sets of data published by Heylen [37], Davies et al. [38], and Urquijo et al. [39] (see Table 1). As visible from Fig. 3c, the data do not follow a linear behavior down to the multiplication threshold, even if the spread of the points is somewhat smaller than for CO₂. Again, we are forced to fit the Korff parameterization only above 100 Td and, correspondingly, the horizontal scale of Fig. 4c can only begin at E/N =100 Td. The present α/N values are in good agreement with the experimental data from the other authors between 100 Td and 150 Td, as it can be seen from Fig. 4c. In general, considering all data sets, large differences of up to 30% are present, but still compatible with the quoted uncertainties. For E/N > 150 Td, the data by Heylen [37] and by Davies et al. [38] tend to get closer, while those by Urquijo et al. [39] and ours are up to 20% above and below, respectively, at the highest field strengths reached. Once more, these differences are still compatible with the quoted uncertainties. The discrepancies found among the experimental data sets cannot be attributed to the techniques used by the authors: only Heylen [37] employed the SST (see Table 1). The difference ($\approx 7\%$) between our α/N values obtained at 120 hPa and 930 hPa, at very close E/N values, are within the quoted overall uncertainty.

The Magboltz simulations follows rather well the average behavior of the data, as represented by the Korff parameterization (i.e., the horizontal line in Fig. 4c). For CH₄, the inclusion of the anisotropies in the cross sections has a very small influence, at most around 1% for E/N around 150 Td, well below the 6% found for N₂ and CO₂. So, again, their inclusion for the E/N range studied here and using data on α/N cannot be supported within present experimental uncertainties.

4.2. First ionization coefficient in the CH₄ – based TEG mixture

After validating the present setup with the data on N₂, CO₂, and CH₄, measurements with the tissue-equivalent gas mixture constituted by CH₄ (64.4%), CO₂ (32.4%), and N₂ (3.2%) were carried out to obtain α/N in the E/N range between 100 Td and 290 Td. The results are presented in Fig. 5 together with those obtained in this work for N₂, CO₂, and CH₄. It is well visible that the mixture behaves quite similarly to its dominant component (CH₄). As a matter of fact, the next most abundant component (CO₂) also has rather close values of α/N and only the minority component (N₂) has much lower ones. Under such conditions (i.e., when the minority component is more difficult to ionize than the dominant one) excitation energy transfer between the different species of molecules in the mixture by molecule-molecule collisions (i.e., the Penning effect) is not expected to alter significantly α/N . This simple observation has been confirmed with detailed simulations performed in cylindrical geometry by Ségur et al. [8] and in a parallel plate configuration by us. The latter authors found that for reduced field strengths less than about 2650 Td, the α/N coefficients in both the methane-based TE gas and pure methane are quite similar.

Since no experimental data on α/N in the CH₄-TEG are available in planar geometry at any field range, the consistency of our results was

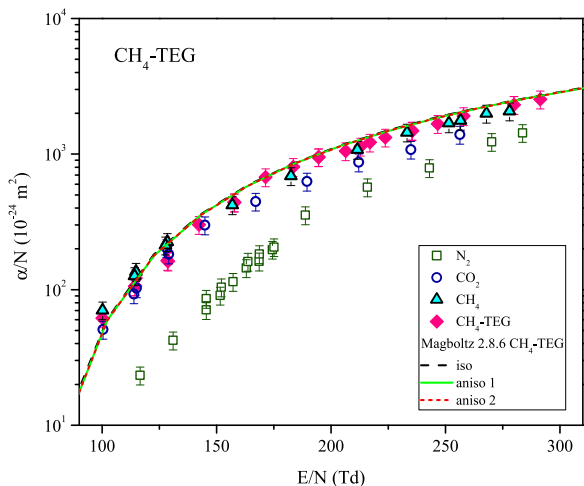


Fig. 5. Density-normalized first Townsend ionization coefficient, α/N , for the CH_4 -TEG mixture as a function of E/N together with Magboltz results (continuous and dashed lines). For comparison, the measurements in each component of the referred TEG mixture are also included.

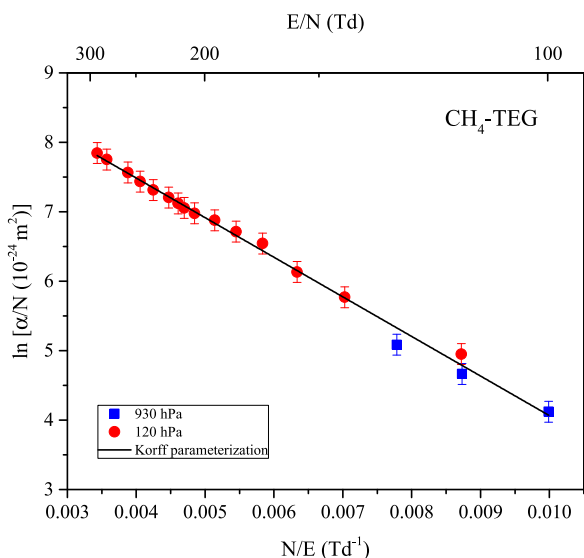


Fig. 6. Korff parameterization fitted to our experimental data on α/N for the CH_4 -TEG. The values for A and B are $(17.4 \pm 1.1) \times 10^{-21} \text{ m}^2$ and $(570 \pm 1) \text{ Td}$, respectively.

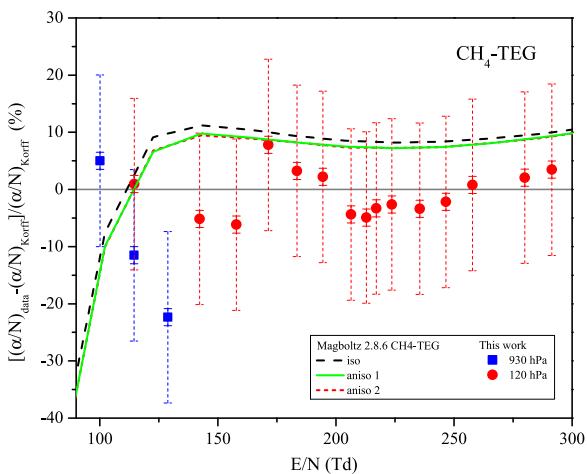


Fig. 7. Residues of the present experimental data on α/N from the fit with the Korff parameterization for the CH_4 -TEG mixture. The error bars represent the total uncertainty (dashed line) and the instrumental uncertainty (full line). The residues of the Magboltz simulations are also included.

checked once more by plotting the logarithm of α/N as a function of N/E , see Fig. 6. It is evident that the experimental results indeed follow a linear behavior down to the multiplication threshold. As in the previous section, a fit with the Korff parameterization allowed us to introduce the residues, see Fig. 7, and show on a rather magnified scale the deviations, which are around 10%. Even if the Korff parameterization has a more semi-empirical than theoretical justification, because there are no other experimental data for the TEG mixture, we discuss the plausibility of the values obtained for the constants A and B: $(17.4 \pm 1.1) \times 10^{-21} \text{ m}^2$ and $(570 \pm 1) \text{ Td}$, respectively. According to a simplified theory of the ionization in gases [40], it is customary to compare the ratio B/A (i.e., $32.7 \pm 2.1 \text{ eV}$ in the present case) with the effective ionization potential (V_i) of this mixture. This V_i value lies between the weighted average ionization potential of CH_4 -TEG (13.08 eV [41]) and the mean energy required for an electron to produce ionization in this mixture (values ranging from 29.60 eV up to 58.61 eV have been reported [42]), thus confirming the general consistency of our measurements.

The results of the Magboltz simulations are also superimposed on Fig. 7. For the case of mixtures, the code has a special flag that allows enabling or disabling the excitation energy transfer in collisions between different species of molecules (i.e., the Penning effect). We tried this option and we did not observe any difference in the values of α/N calculated by the code, confirming what was discussed on general grounds above. The inclusion of anisotropies has a small effect, in agreement with what has been observed for the majority component (CH_4) in the previous section. The simulation follows the general trend of the data, possibly overestimating their absolute value by 5–10% at higher E/N , but this is currently at the limit of our experimental uncertainties. As observed for all the mixture components, except the minority one (N_2), close to the multiplication threshold the simulation underestimates markedly the data and does not follow the linear behavior of the Korff parameterization.

As mentioned, only one set of data for α/N was previously published by Schmitz and Booz [7] for the TEG mixture, it is compared with our in Fig. 8. They employed a Rossi type proportional counter with a central wire coaxially surrounded by a helix to guarantee the cylindrical symmetry of the electric field in the vicinity of the wire. In

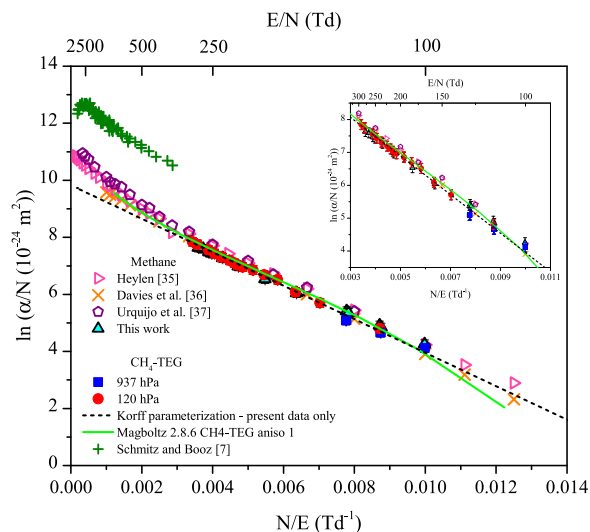


Fig. 8. Linearized representation of $\ln(\alpha/N)$ versus N/E for the CH_4 -TEG mixture. Our data are compared with those obtained by Schmitz and Booz with a proportional counter at much higher values of E/N . Because it is expected (see the text) that the CH_4 -TEG mixture follows approximately the behavior of the majority component, CH_4 , the results for the latter (ours and those from the literature) are also displayed. The fit with the Korff parameterization to our data alone and the results of simulations performed with the Magboltz code are also included for completeness. Finally, the E/N region of the present data (100–300 Td) is shown expanded in the inset.

this experiment, α/p values were obtained from measurements of gas gain as a function of pressure-normalized field strengths (E/p) between 110–1780 V cm⁻¹ torr⁻¹. As their results were published in the form of a graph (α/p versus E/p), the coordinates of the data points were obtained by us through a digitization procedure. The α/p values were converted by us to α/N , as well as the values of E/p to E/N given in Td. By looking at Fig. 8, it is clear that the data from Schmitz and Booz [7] were obtained in the very high E/N region (315–5045 Td) without any overlap with the field range covered in this work. The values of α/N in pure methane published by Heylen [37], Davies et al. [38], and Urquijo et al. [39] were also included in this figure to demonstrate that, while our data are close to those on the majority component obtained by other authors, those by Schmitz and Booz are approximately 20% higher. As discussed above, the Penning effect cannot produce an increase of the first ionization coefficient in the TEG mixture above the value of CH₄. If the Korff parameterization, adjusted to our data, is used to extrapolate their behavior at higher E/N , an approximate consistency with the mentioned values by Heylen, Davies et al., and Urquijo et al. for CH₄ is indeed found. So it is not possible to avoid the conclusion that there is a large disagreement between our data and those from Schmitz and Booz, even if they cover non overlapping E/N ranges. It seems reasonable to assume that the α/p values by Schmitz and Booz [7] were influenced by some other effect not present in a parallel plate geometry.

The standard analysis of the gas multiplication [43] suggests a possible lack of equilibrium between the accelerated electrons and the electric field due to the strong field gradient near the anode in cylindrical geometry. Under such a condition, which is especially pronounced at high fields and at low pressures, the energy gained by the electrons between successive collisions is smaller than that they would acquire if the field would be uniform [3]. However, as demonstrated by Ségur et al. [8] and Mitev et al. [43], regardless of the electric field being uniform or not, the presence of non-equilibrium effects diminishes the gas gain and therefore, the first ionization coefficient. A further factor influencing the gas multiplication in a cylindrical proportional counter must be considered when the motion of electrons is not strictly radial. Mainly at low pressures, some of electrons may circle the wire undergoing more collisions before being collected by the anode. Unlike the non-equilibrium effects, this leads to an experimental gas gain higher than expected in a uniform electric field. Because of all these complexities affecting the gas gain in a counter with a cylindrical geometry, it is not surprising that the results by Schmidt and Booz [7] diverged from ours.

5. Conclusions

Data on the density normalized first Townsend ionization coefficient, α/N , in the methane-based TEG mixture (CH₄ – 64.4%, CO₂ – 32.4%, and N₂ – 3.2%), gathered for E/N between 100 Td and 290 Td, have been presented for the first time. This extended E/N range was achieved owing to the improvements done in our previous setup to allow decreasing the gas pressure from 930 hPa down to 120 hPa. The method used to obtain α/N is based on the measurement, as a function of E/N , of the ionization current growth in a parallel plate geometry and in a pulsed irradiation regime. The theoretical validation of this method applied at field strengths higher than 200 Td was accomplished through an investigation on the correspondence of the transport parameters obtained with the Magboltz simulation code in the PT and SST regimes. From these studies, for reduced field strengths up to 300 Td, the difference among the parameters defined in the SST and PT conditions is expected to be at most around 10%.

The validation of the present apparatus was performed with the data on α/N obtained in N₂, CO₂, and CH₄. Indeed, the whole set of α/N measurements performed in the latter gases at atmospheric and low pressures agreed with earlier published data and Magboltz calculations. Great care has been devoted to keep the ohmic drop across the glass

anode below 1% of the applied voltage even in the worst case (atmospheric pressure and high E/N) by the aid of calibrated attenuators of the laser beam. For this reason, this effect was neglected in this work and E/N values were not corrected for.

A comparison between experimental values available in the literature and ours has been performed for N₂, CO₂, and CH₄, representing the residues from a Korff parameterization fitted to all selected points. This enabled us to analyze deviations smaller than those visible on the usual logarithmic plot of α/N versus E/N . Despite the apparent conceptual simplicity of the various methods available to measure the first Townsend ionization coefficient, it is not uncommon to find values from different authors that disagree by as much as 20%, even for recent publications.

Since no experimental results are available in planar geometry for the CH₄-based TEG mixture at any field range, the measurements were compared with those for the components alone. It was found that the mixture behaves quite similarly to the majority one. This was indeed predicted by Ségur et al., who performed detailed simulations, and can be understood in simple terms by considering that the second most abundant component has a similar α/N and, finally, the minority one is much harder to ionize: under these conditions, the excitation energy transfer in molecule-molecule collisions (i.e., the Penning effect) cannot alter α/N significantly. The Korff parameterization was also employed to discuss the consistency of our results. The values obtained for the constants A and B, and therefore, the effective ionization potential (V_i) of this mixture, are in accordance with the values expected from the approximate theory of ionization in gases. A good agreement has also been found with Magboltz calculations.

Acknowledgments

The authors are deeply grateful to Dr. M. M. R. Fraga (in memoriam) from LIP-Coimbra, Portugal, for valuable discussions on the low-pressure gas system, crucial for the development of this work. Thanks are also due to Dr. P. Fonte (LIP-Coimbra, Portugal) for many helpful discussions and the free supply of the glass slabs. The assistance of A. M. A. Pereira (LIP-Coimbra, Portugal) concerning low-pressure operation is acknowledged. A. R. Petri would like to thank CNPq for the award of a scholarship. This work was co-financed by FAPESP under Contracts 02/04697-1, 07/50591-4, 09/51809-9, and by CNPq via Contracts 478859/2009-0 and 479079/2010-2.

Appendix A. Supplementary material

Supplementary data associated with this article can be found in the online version at doi:10.1016/j.nima.2017.01.007.

References

- [1] H.H. Rossi, M. Zaider, *Med. Phys.* 18 (1991) 1085.
- [2] H.H. Rossi, W. Rosenzweig, *Radiology* 64 (1955) 404.
- [3] H.H. Rossi, M. Zaider, *Microdosimetry and its Applications*, Springer-Verlag, Berlin Heidelberg, New York, 1996.
- [4] International Commission on Radiation Units and Measurements, *Microdosimetry*, ICRU Report no. 36, 1983.
- [5] M. Farahmand, A.J.J. Bos, C.W.E. van Eijk, *Nucl. Instrum. Methods A* 506 (2003) 160.
- [6] P. Kliauga, A.J. Walker, J. Barthe, *Radiat. Prot. Dosim.* 61 (1995) 309.
- [7] T. Schmitz, J. Booz, *Radiat. Prot. Dosim.* 29 (1989) 31.
- [8] P. Ségur, I. Pérès, J.P. Boeuf, M.C. Bordage, *Radiat. Prot. Dosim.* 29 (1989) 23.
- [9] P. Fonte, A. Mangiarotti, S. Botelho, J.A.C. Gonçalves, M.A. Ridenti, C.C. Bueno, *Nucl. Instrum. Methods A* 613 (2010) 40.
- [10] I.B. Lima, A. Mangiarotti, T.C. Vivaldini, J.A.C. Gonçalves, S. Botelho, P. Fonte, J. Takahashi, L.V. Tarelho, C.C. Bueno, *Nucl. Instrum. Methods A* 670 (2012) 55.
- [11] A. Mangiarotti, I.B. Lima, T.C. Vivaldini, J.A.C. Gonçalves, A.R. Petri, S. Botelho, P. Fonte, C.C. Bueno, *Nucl. Instrum. Methods A* 694 (2012) 162.
- [12] R. Santonico, R. Cardarelli, *Nucl. Instrum. Methods A* 187 (1981) 377.
- [13] R. Cardarelli, R. Santonico, A. di Biagio, A. Lucci, *Nucl. Instrum. Methods A* 263 (1988) 20.
- [14] M. Abbrescia, *Nucl. Instrum. Methods A* 533 (2004) 7.
- [15] D. González-Días, P. Fonte, J.A. Garzón, A. Mangiarotti, *Nucl. Phys. B* 158 (2006)

- 111 (Proc. Suppl.).
- [16] C.C. Bueno, M.M. Fraga, J.A.C. Gonçalves, R. Ferreira Marques, A.J.P.L. Policarpo, M. Damy de S. Santos, Nucl. Instrum. Methods A 408 (1998) 496.
- [17] M.M. Fraga, R. Ferreira Marques, Y. Ivaniouchenkov, E.P. de Lima, F. Neves, A.J.P.L. Policarpo, C.C. Bueno, J.A.C. Gonçalves, M. Damy, de, S. Santos, L. Costa, S. Mendiratta, J.H. Monteiro, Nucl. Instrum. Methods A 419 (1998) 485.
- [18] M.M. Fraga, E.P. de Lima, R. Ferreira Marques, A.J.P.L. Policarpo, C.C. Bueno, J.A.C. Gonçalves, M. Damy de S. Santos, IEEE Trans. Nucl. Sci. 45 (1998) 263.
- [19] S. Biagi, Nucl. Instrum. Methods A 273 (1988) 533.
- [20] S. Biagi, Nucl. Instrum. Methods A 283 (1989) 716.
- [21] S. Biagi, Nucl. Instrum. Methods A 421 (1999) 234.
- [22] S. Biagi, Magboltz, the Fortran source code of the standalone version is freely downloadable from (<http://consult.cern.ch/writeup/magboltz/>), 2016.
- [23] C.B. Opal, W.K. Peterson, E.C. Beaty, J. Phys. Chem. 55 (1971) 4100.
- [24] S. Longo, M. Capitelli, Plasma Chem. Plasma Process. 14 (1994) 1.
- [25] A. Okhrimovskyy, A. Bogaerts, R. Gijbels, Phys. Rev. E 65 (2002) 037402.
- [26] Y. Sakai, H. Tagashira, S. Sakamoto, J. Phys. D: Appl. Phys. 10 (1977) 1035.
- [27] H. Tagashira, Y. Sakai, S. Sakamoto, J. Phys. D: Appl. Phys. 10 (1977) 1051.
- [28] A. Mangiarotti, A Theoretical Study of the Fast Signal Induced by Avalanche Growth in Pure Nitrogen and Pure Isobutane, Activity Report of Project FAPESP 07/50591-4
- [29] S.A. Korff, Electron and Nuclear Counters, D. Van Nostrand Company, New York, 1946.
- [30] F. Sauli, Principles of operation of multiwire proportional and drift chambers, Yellow Report CERN, 1977, pp.77–09.
- [31] S.C. Haydon, O.M. Williams, J. Phys. B: At. Mol. Phys. 9 (1976) 523.
- [32] M. Yousfi, J. de Urquijo, A. Juárez, E. Basurto, J.L. Hernández-Ávila, IEEE Trans. Plasma Sci. 37 (2009) 764.
- [33] D. Dahl, T. Teich, C. Franck, J. Phys. D: Appl. Phys. 45 (2012) 485201.
- [34] J.L. Hernández-Ávila, E. Basurto, J. de Urquijo, J. Phys. D: Appl. Phys. 35 (2002) 2264.
- [35] M.S. Bhalla, J.D. Craggs, Proc. Phys. Soc. 76 (1960) 369.
- [36] V.J. Conti, A.W. Williams, J. Phys. D: Appl. Phys. 8 (1975) 2198.
- [37] A.E.D. Heylen, J. Chem. Phys. 38 (1963) 765.
- [38] D.K. Davies, L.E. Kline, W.E. Bies, J. Appl. Phys. 85 (1989) 3311.
- [39] J. de Urquijo, C.A. Arriaga, C. Cisneiros, I. Alvarez, J. Phys. D: Appl. Phys. 32 (1999) 41.
- [40] A. von Engel, Ionized Gases, Second ed., Clarendon Press, Oxford, 1965.
- [41] National Institute of Standards and Technology (<http://webbook.nist.gov/chemistry/>) (2016).
- [42] E. Waibel, B. Grosswendt, Phys. Med. Biol. 37 (1992) 1127.
- [43] K. Mitev, P. Ségur, A. Alkaa, M.C. Bordage, C. Furstoss, C. Khamphan, L. De Nardo, V. Conte, P. Colautti, Nucl. Instrum. Methods A 538 (2005) 672.